# Efficient Non-Linear Idealisations of Aircraft Fuselage Panels in Compression

Murphy, A., Price, M., Gibson, A., & Armstrong, C. (2004). Efficient Non-Linear Idealisations of Aircraft Fuselage Panels in Compression. *Finite Elements in Analysis and Design*, *40*(13-14), 1977-1993.
https://doi.org/10.1016/j.finel.2003.11.009

**Published in:**
Finite Elements in Analysis and Design

**Document Version:**
Peer reviewed version

# EFFICIENT NON-LINEAR IDEALISATIONS OF AIRCRAFT FUSELAGE PANELS IN COMPRESSION

A. Murphy[1], M. Price[2], A. Gibson[2], C.G. Armstrong[3]

1 – Corresponding Author: School of Aeronautical Engineering, Queen's University Belfast, Belfast, N. Ireland. (E-mail: a.murphy@qub.ac.uk, Tel: +44 (0) 28 9027 4095, Fax: +44 (0) 28 9038 2701)

2 – School of Aeronautical Engineering, Queen's University Belfast, Belfast, N. Ireland.

3 – School of Mechanical Engineering, Queen's University Belfast, Belfast, N. Ireland.

**Abstract**

Aircraft fuselages are complex assemblies of thousands of components and as a result simulation models are highly idealised. In the typical design process, a coarse FE model is used to determine loads within the structure. The size of the model and number of load cases necessitates that only linear static behaviour is considered. This paper reports on the development of a modelling approach to increase the accuracy of the global model, accounting for variations in stiffness due to non-linear structural behaviour. The strategy is based on representing a fuselage sub-section with a single non-linear element. Large portions of fuselage structure are represented by connecting these non-linear elements together to form a framework. The non-linear models are very efficient, reducing computational time significantly.

**Keywords:** Fuselage barrel analysis, Post buckling stiffness, Non-linear modelling

## 1 Introduction

During a conventional fuselage design process, the preliminary detail design stage generates a highly idealised representation of the global fuselage structure. This design is then iteratively improved to satisfy performance criteria and regulatory requirements. At this stage a Finite Element model is constructed from this data, Figure 1, in which the philosophy is to model the structure with sufficient detail to evaluate the internal loads. In general, the aircraft fuselage is discretised to a single element between each stringer and each frame. This is the global or loads model, and is analysed for all critical aircraft loading cases. There are normally between two and three hundred loading cases from which the critical loads are determined.

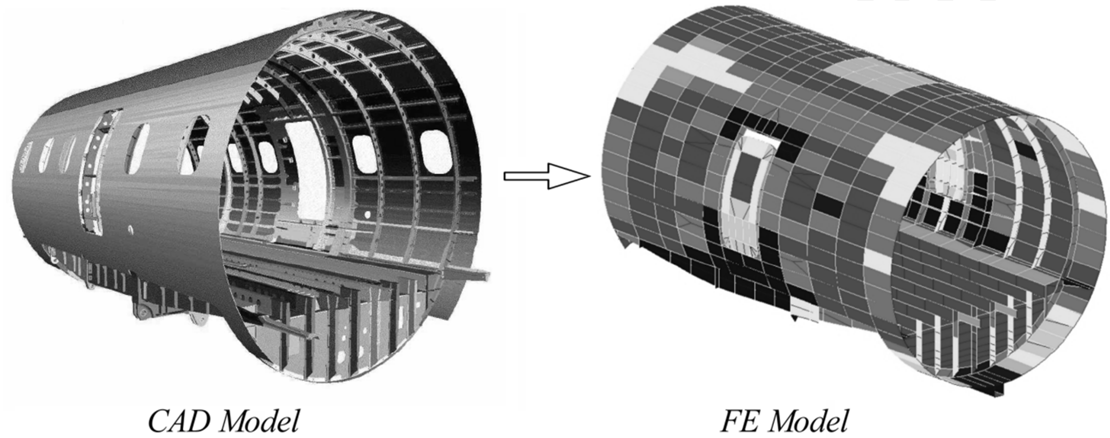


Figure 1 – Highly idealised global fuselage barrel model

The primary aim of this global analysis is to obtain load paths and load levels throughout the structure. The loads obtained from the global model are then used to carry out detailed stressing on individual components. The structural members are stressed using conventional methods, where in the case of buckling analysis the techniques are based on the empirical/semi-empirical methods presented in Bruhn [1], NASA Astronautics Structures Manual [2], and the ESDU Structures Sub-series [3]. The Finite Element global analysis is linear static and non-linear geometry and material behaviour is only considered at the detailed stressing phase, the results of which are not fed back into the global model.

Finite Element tools are now being developed to improve the accuracy and reliability of stiffened panel empirical/semi-empirical buckling and collapse analysis methods, with some success in improving accuracy [4, 5, 6]. However, modelling and analysis times are still excessive and cannot yet replace existing approaches [4, 5, 6]. Both sub-structuring [7] and sub-modelling [8, 9] are common techniques used in linear type analysis problems to reduce analysis costs [10]. Sub-structuring allows a collection of model elements to be grouped together and replaced within the model with a sub-structure or a super-element. All but retained boundary degrees of freedom are eliminated on the basis of a linear response from the grouped elements. A sub-structure or super-element appears to the rest of the model simply as a stiffness. Sub-modelling is a technique used to study a local region of a model with a refined mesh, based on interpolation of a solution from an initial, relatively coarse, global model. Sub-modelling is most useful when it is necessary to obtain an accurate, detailed solution in a local region and the detailed modelling of that local region has negligible effect on the overall global solution.

The difference between sub-structuring and sub-modelling is that in sub-structuring equilibrium is enforced between the super-elements and the global model. Whereas with sub-modelling there is no guarantee that the local model stresses generated by 'driven' node displacement will be in equilibrium with stresses in the global model. The main limitation with sub-structuring, for non-linear barrel analysis, is that super-element response to loading must be linear. The main limitation with sub-modelling is interpolating global analysis data from an equilibrium stepping analysis to a sub-model to perform another equilibrium stepping analysis, where the local region response affects the overall global response.

Alternative mesh-refinement [11, 12] procedures may be used to reduce analysis costs for linear problems. However it is worth noting that the general mesh-refinement approach increases the density of elements within a critical region of the model; this reduces the stiffness of the local region and may falsely induce buckling prematurely within the refined area, generating inaccurate results. Alternatively, the reduced local stiffness may alter component load paths and load magnitudes, leading to inaccurate stressing of sub-regions and again generating inappropriate results [12].

The strategy presented here is based on modelling a typical fuselage stiffened panel sub-section, Figure 2, with a single non-linear element. A typical sub-section is taken to be a stringer segment with attached skin covering one half bay either side of the stringer and the segment length covers one full frame bay. Each non-linear element is required to capture both geometric and material non-linearity in its response. The non-linear data can be obtained from detailed Finite Element simulation or experimental testing of a sub-section. The whole fuselage model then becomes a collection of such non-linear elements and is capable of accurately assessing the compression behaviour of the fuselage.

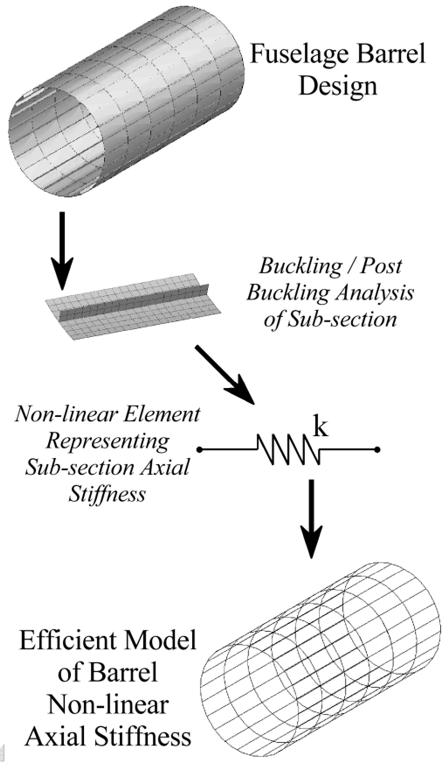


Figure 2 – Fuselage barrel modelling strategy

The procedure followed here is to carry out detailed FE analysis on individual sub-sections to generate the non-linear model data and then to carry out an analysis of the newly assembled global model. Since the execution time for buckling analysis rapidly increases with model size [5], the analysis of all the individual sub-sections is still less than that for the complete structure. Moreover since there is a significant degree of repeatability in the structure not every sub-section needs to be analysed.

The following section describes the procedure for obtaining the non-linear data for a single non-linear element before describing how the global model is assembled and analysed. The global structure used as a benchmark for this work is a 36 by 34 inch flat fuselage panel used in a previous study [4] on the post buckling behaviour of fuselage panels. This naturally provided a basis since both detailed FE and experimental results already exist for comparison with this new modelling approach.

## 2 Sub-Section Modelling

A number of element types were considered as possible 1D non-linear entities, including beam elements with modified stress-strain data and spring elements with non-linear force displacement response properties [13]. Both element types produce identical output with the same input stiffness properties; however using spring elements required a minimum amount of data manipulation. Using a spring element as a 'non-linear super element' the non-linear axial stiffness of the sub-section may be effectively modelled as a single spring. The major advantage of a non-linear spring element over conventional sub-structuring is that it is able to represent a structure's non-linear response to loading whereas conventional sub-structuring is limited to linear cases. The main concern to be addressed is then the generation of the spring input data.

A number of approaches may be used to generate the stiffness response including theoretical, numerical and experimental analysis methods [13]. The technique presented within this paper focuses on the use of non-linear 3D-Shell FE models to generate the required stiffness data since these have already been successfully used for panel collapse analysis [14, 15].

Stiffened panels are commonly modelled as a series of shell elements representing the plate sections and beam elements representing the stiffener sections, Figure 3a. This level of idealisation will accurately and efficiently represent the structure's linear stiffness but will fail to capture stiffener local cross-section translation and rotations and therefore fail to accurately model non-linear buckling and post buckling behaviour [4, 6, 16]. In order to predict the collapse behaviour the cross-section must be modelled in detail [15].

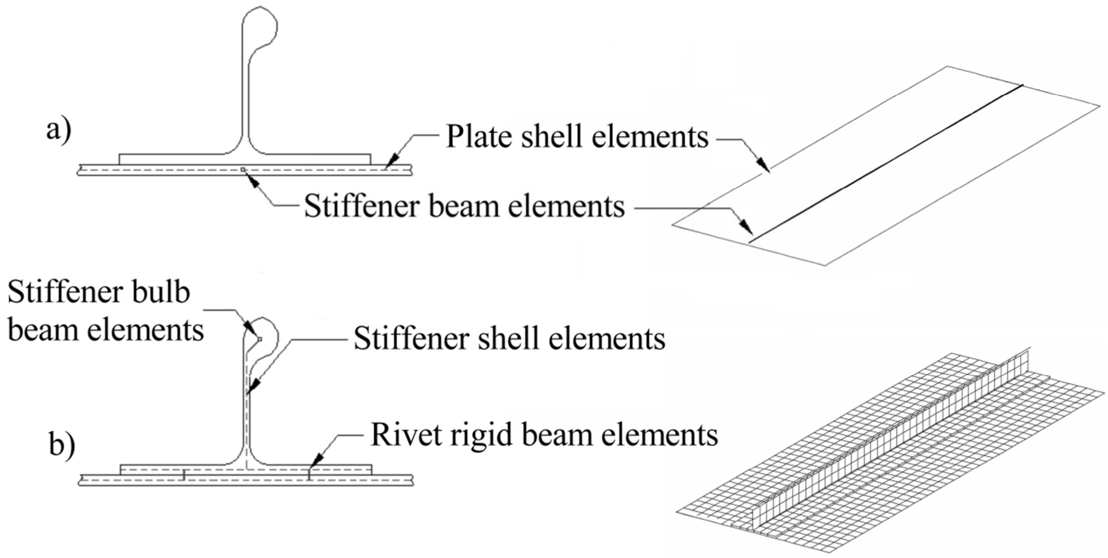


Figure 3 – Stiffener idealisation

Lynch [4] developed a number of Finite Element modelling methodologies for the buckling and post buckling analysis of metallic fuselage panels. The idealisations proposed focus on modelling each section of the stiffener cross-sections with shell or beam elements, Figure 3b. The work investigated element selection, minimum required mesh density and the plate-stiffener interface idealisation. The work developed a computationally expensive analysis methodology capable of accurately predicting the structural response of flat fuselage stiffened panels loaded in compression. The skin-rivet-stringer joint idealisation represents the rivets with rigid links (MPCs) Figure 3b. The contact condition between the skin and the stringer flange is not modelled here as the computational costs have been shown to outweigh the small increase in model stiffness prediction accuracy [4].

Following the computational methodologies developed by Lynch and applying appropriate boundary conditions, which aim to match the true constraint conditions within the global structure, the required sub-section stiffness data can be generated. It should be noted however that the applied sub-section boundary conditions are based on the same simplifying assumptions followed as part of the conservative traditional analysis process [1, 2, 3]. The model results will therefore tend towards under predicting the structure's response [4]. An example of a typical sub-section model and its associated boundary conditions is detailed in Figure 4. A uniform axial displacement is applied to the upper end of each sub-section model with the lower end axial displacement constrained, both the upper and lower model edges are assumed to be simply supported [1]. The simple support sub-section boundaries, constraint skin and stringer out-of-plane deformations along the frame lines, this out-of-plane condition represents the post-buckling constraint within the global structure. The simple support conditions however, do not account for frame rotational constraints and hence the conservative response noted above. The model side edge nodes have material constraints applied to replicate their constraint conditions within the global structure, Figure 4. Within the post-buckling region the material constraints applied to the side nodes permits skin out-of-plane deformations, allowing skin post-buckling out-of-plane behaviour.

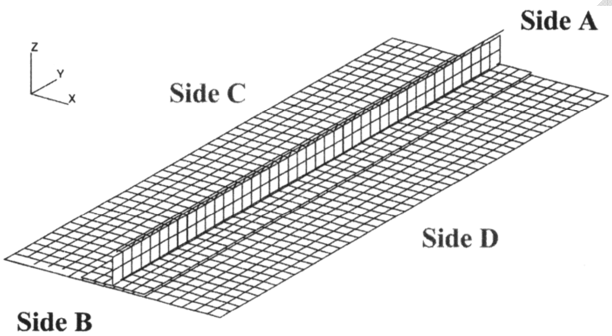


| ***Boundary Conditions Table*** | |
|---|---|
| ***Side A*** | 1) Negative uniform Y-Axis displacement (model loading)<br>2) Z-Axis translations restrained (in-plane) |
| ***Side B*** | 1) Y-Axis translations restrained (rigid body restraint)<br>2) Z-Axis translations restrained (in-plane) |
| ***Side C*** | 1) X-Axis translations restrained (material constraints)<br>2) Y-Axis rotations restrained (material constraints) |
| ***Side D*** | 1) X-Axis translations restrained (material constraints)<br>2) Y-Axis rotations restrained (material constraints) |

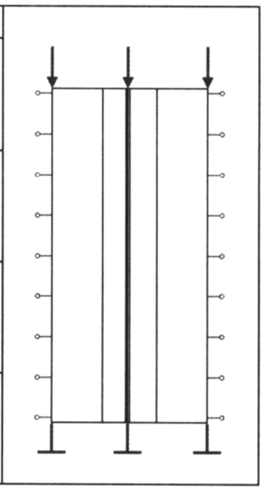

Figure 4 – Sub-Section model boundary conditions

Based on the results of extensive element mesh convergence studies [4], linear quadratic shell elements, ABAQUS element S4R [17], with a minimum mesh density of 4 nodes per buckle half-wave was used for each sub-section model. The sub-section models were analysed for linear buckling, extracting the fundamental eigenmode in each case. Each model was then seeded with an initial geometric imperfection based on the sub-section's fundamental eigenmode, with a maximum magnitude of 10% skin thickness [4]. Post buckling behaviour was then determined accounting for both material and geometric non-linearity employing a Newton-Raphson solution procedure [17, 18]. The sub-section axial stiffness was then extracted for the analysis data. Figure 5 illustrates a typical sub-section axial load versus axial deflection curve predicted by a sub-section FE analysis.

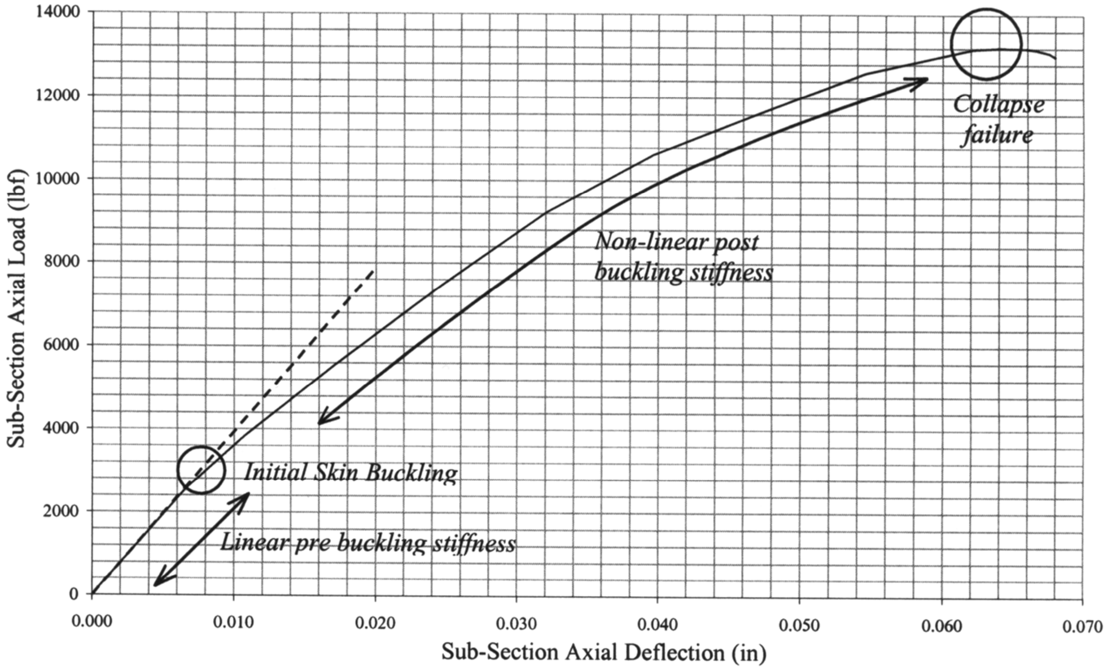


Figure 5 – Sub-Section model axial stiffness

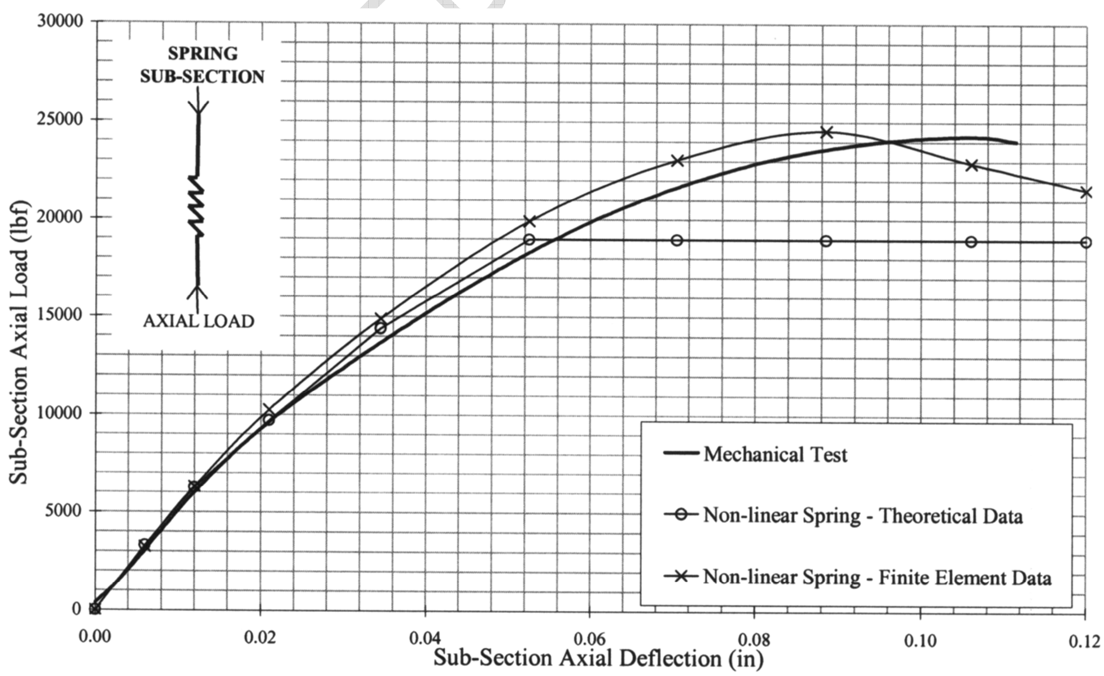


Figure 6 – Non-linear spring results [13]

Murphy [13] considered sub-section data generated using theoretical analysis as well as detailed 3D-Shell FE models. The sub-structuring procedure detailed above was then validated against experimental sub-section specimen tests. The load-deflection curves for these cases are illustrated in Figure 6. It is worth noting that the discrepancy between the experimental load-deflection curve and the non-linear spring model curves is due primarily to the under design of edge support bars used in the experimental set-up, Murphy [13]. The work demonstrated that the spring non-linear sub-structuring technique detailed above might be used to accurately model sub-section axial stiffness at a fraction of the cost of detail 3D-Shell modelling techniques. The detailed model took approximately 5 hrs to run[1], whilst having obtained the load-deflection data for the spring analysis run-time was reduced to 30 seconds. It was noted that the true value of the non-linear sub-structuring methods would only be achieved when using non-linear spring elements to model large stiffened panel structures.

Once the sub-section model has been analysed the next stage is the discretisation of the structure's axial load versus axial deflection curve into non-linear spring input data. In practice this is simply a list of load-deflection points entered as spring properties within an analysis input deck [17].

Once all the sub-sections of the global structure are modelled and the spring data generated, the next stage is the assembly of the global spring framework model.

## 3 Assembling the Global Model

The global modelling scheme requires the assembly of the sub-section spring elements in their appropriate location and additionally to account for the lateral and longitudinal interaction between springs via the frame structure. A global model built with the sub-section axial spring elements will only be capable of modelling axial behaviour since this is the only degree of freedom considered in generating the spring data. Therefore any frame local-axial stiffness representation added at the global model stage will not add to the value of the model. Considering the 1D axial nature of the non-linear spring elements used to model sub-sections the fuselage frames are

[1] Analysis preformed on a Silicon Graphics Indigo workstation with 64MB of RAM.

simply modelled as rigid bodies that are free to translate axially, Figure 7. The frames are also constrained from translations normal to the skin, which is consistent with fuselage frame design philosophy [19] and the boundary conditions applied to the sub-section models. Each sub-section spring is attached to the forward and rearward frame structure, this method of coupling the non-linear spring elements although simple, is effective as shall be demonstrated in the next section.

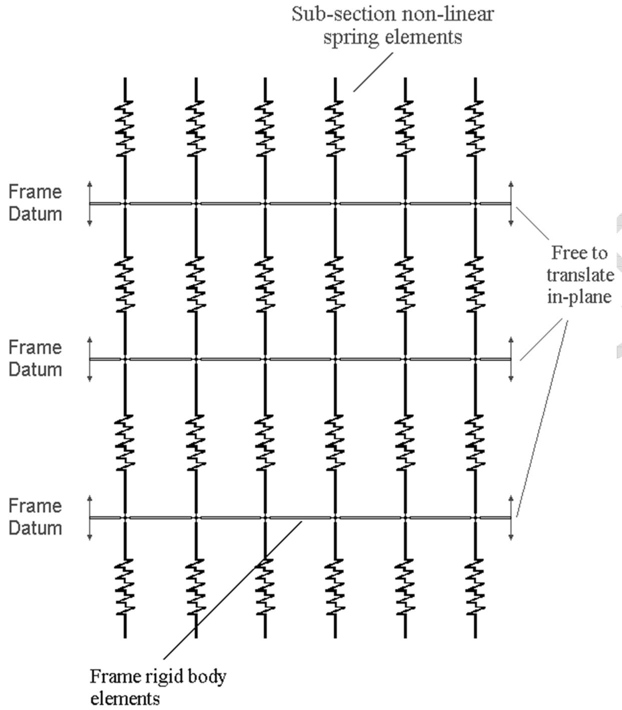


Figure 7 – Global spring framework modelling scheme

## 4 Validation specimen analysis

In order to assess the accuracy and cost of the global stiffness modelling methods, the flat specimen detailed in Figure 8 was analysed and stiffness results compared with detail 3D-Shell FE analysis data and experimental test data. The specimen consists of a 36 by 34 inch skin, stiffened by six stringers and two frame segments. The specimen was designed such that the failure load is approximately three times the initial buckling load of the centre skin bays. The rivet pitch was chosen so as to eliminate inter-rivet buckling. The evaluated buckling load for the centre skin bays was 22,714 lbf (with the edge skin bays buckling at 10,035 lbf) and the theoretical local-flexural failure load was 72,016 lbf. Two specimens were tested in an Avery hydraulic compression-testing machine with a 150-ton capacity, Figure 9. A half-inch thick cerrobend[2] base was cast on to specimens, design to produce fully clamped boundary conditions at each end. The ends were subsequently machined flat and perpendicular to the skin to ensure that uniform axial loads were applied. Frame support fixtures were designed to eliminate frame out-of-plane deflections, while allowing axial displacements. This was achieved by bolting specially built trolleys onto the protruding specimens frames. The trolleys then rolled vertically between support tracks.

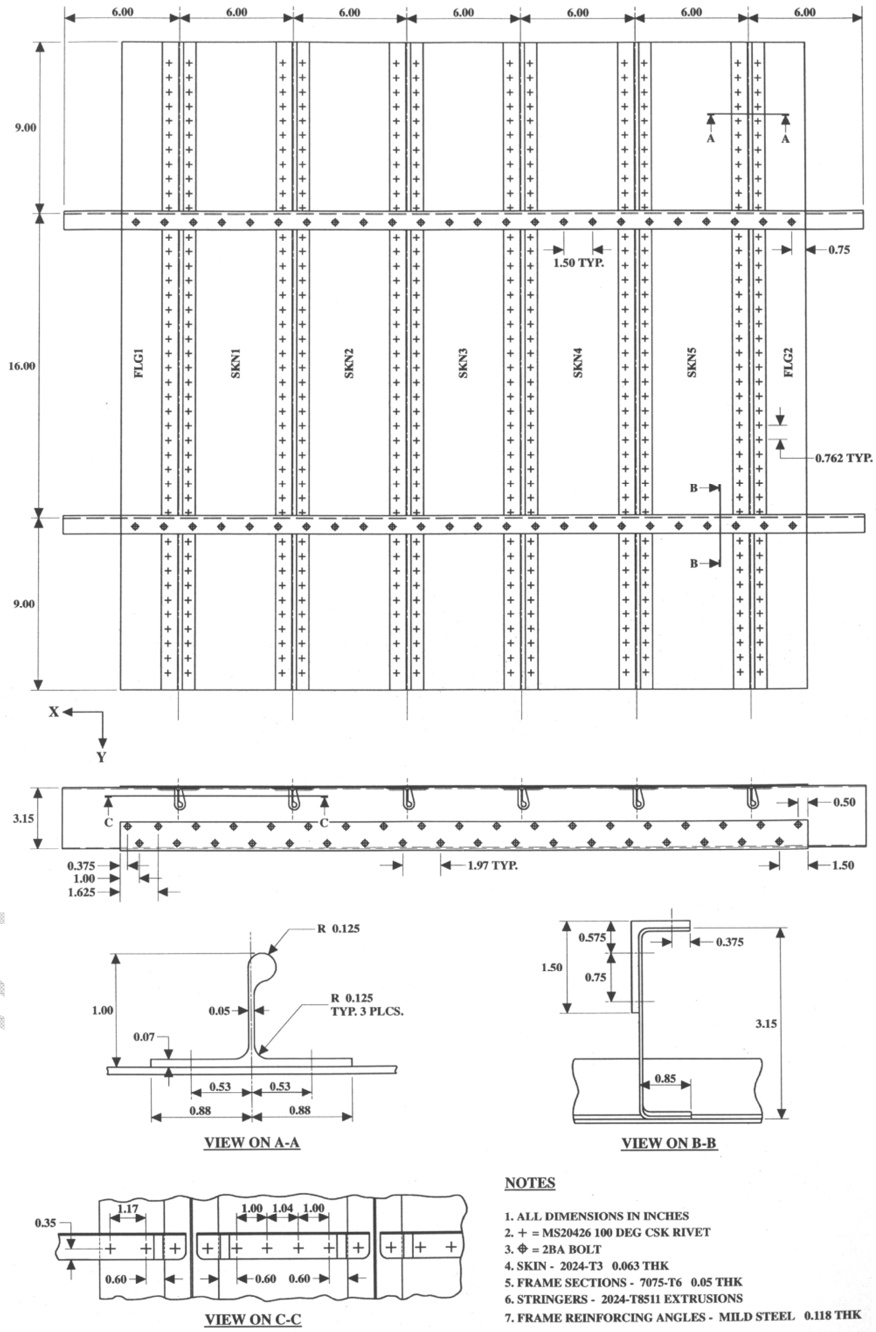


Figure 8 – Validation specimen

[2] Cerrobends is a low melting point alloy used in structural testing to create support bound conditions.

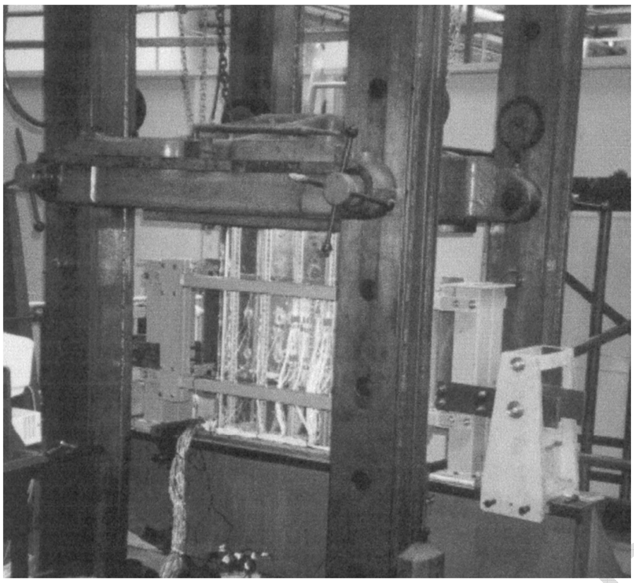

Figure 9 – Test set-up (Avery compression testing machine)

A full non-linear analysis of the specimen was also performed using the 3D-Shell modelling methods outlined in Section 2. The detailed specimen FE analysis modelled non-linear material and geometric behaviour and consisted of approximately 16,000 first order beam and shell elements plus 600 rigid beam elements representing the specimen rivets. The model required three man-days to build and in its completed state consisted of approximately 90,000 degrees of freedom, Figure 10. The loads and boundary conditions applied to the full specimen model were designed to be as representative of the experimental test as possible, Figure 10.

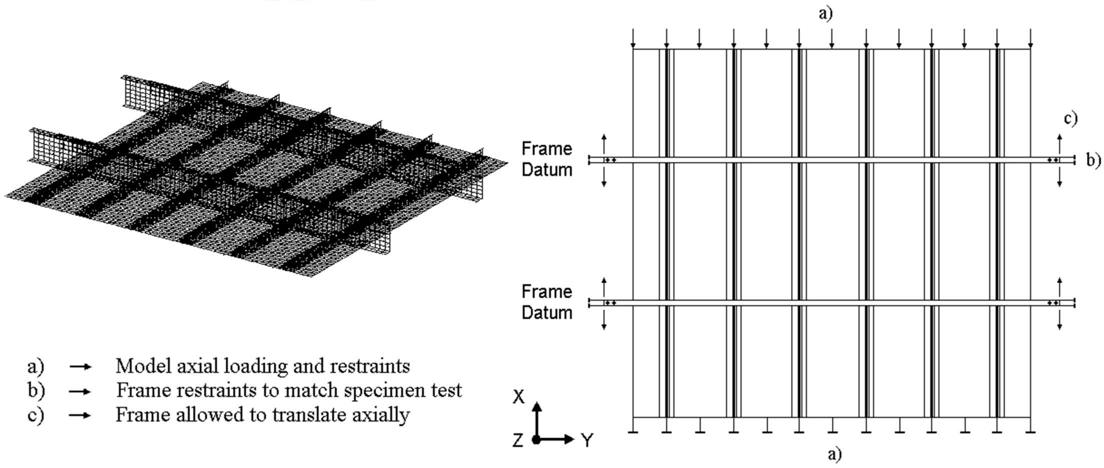


Figure 10 – Specimen FE model plus loading and boundary conditions

The first step in the analysis of the specimen using the non-linear springs is the division of the structure geometry into sub-sections. Each frame bay is divided into a series of sub-sections along the centre skin lines, Figure 11 details the sub-division. The specimen analysis only requires 9 sub-section models considering structural repetition, Figure 11. A sub-section model is required for each geometry set (top, middle and bottom sub-sections) and each geometry model must be analysed for a series of boundary conditions (left, centre, and right sub-sections). In total, 50% of specimen geometry is modelled. Once the structure has been sub-divided the sub-section models may be built and analysed following the procedures laid out in Section 2. For the sub-section at the boundaries of the validation specimens, edges which are free are modelled as free edges and edges clamped in cerrobends are modelled with skin out-of-plane translations constrained and with loading translations free. The resulting axial loads versus deflection curves for the nine sub-models are presented in Figure 12.

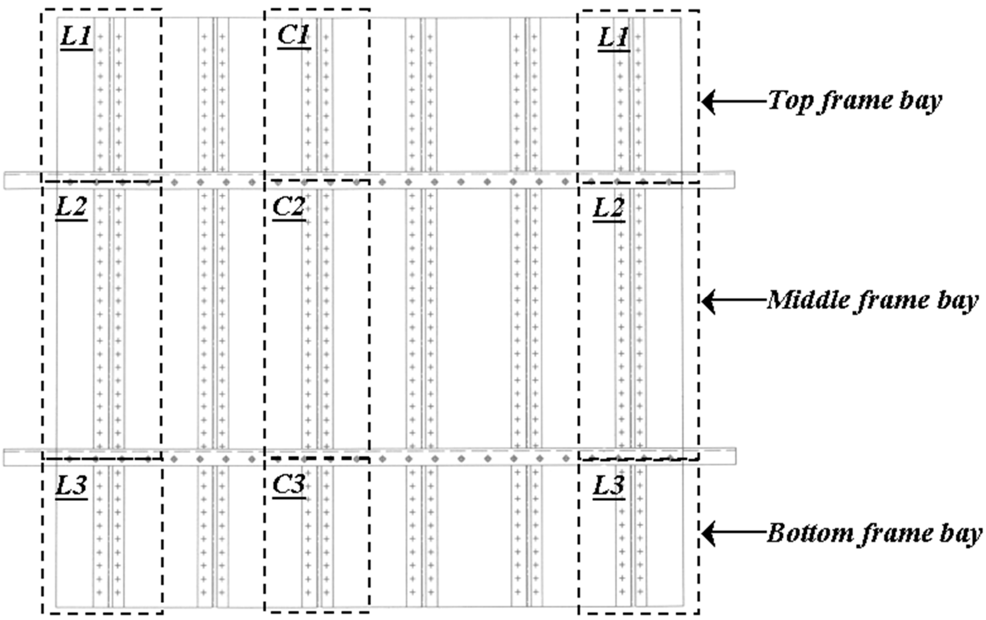


L1 - Sub-Section 1

C1 - Sub-Section 2

R1 - Sub-Section 3

L2 - Sub-Section 4

C2 - Sub-Section 5

R2 - Sub-Section 6

L3 - Sub-Section 7

C3 - Sub-Section 8

R3 - Sub-Section 9

Figure 11 – Specimen sub-division scheme

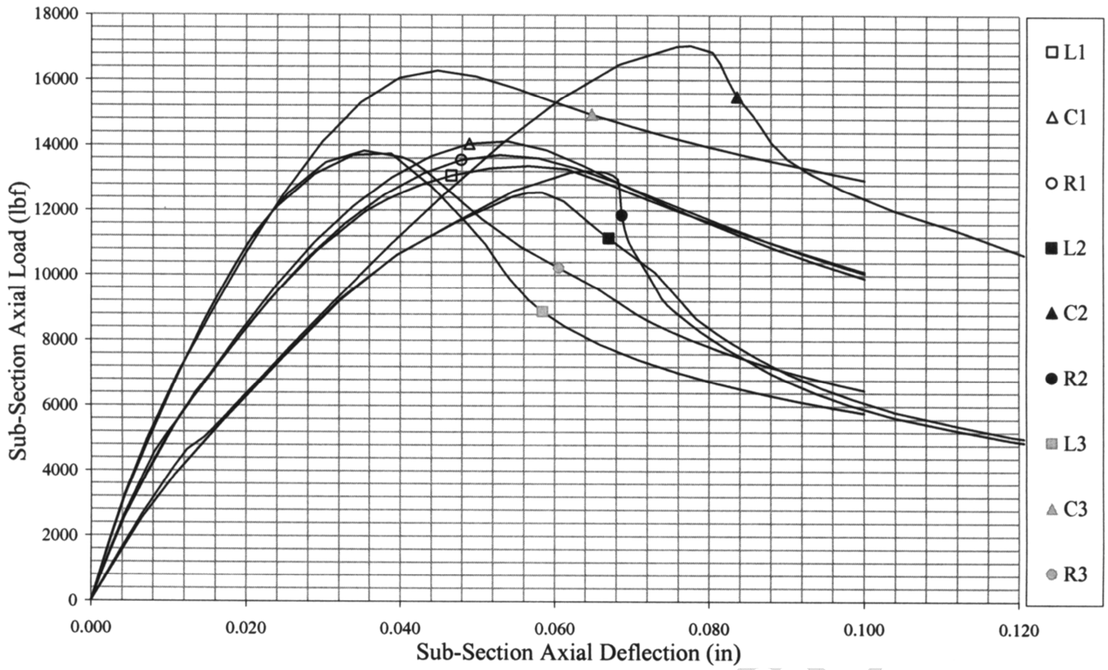


Figure 12 – Specimen sub-section analysis results

Considering Figure 12 there are three distinct groups of curves, one for the top frame bay sub-models (L1, C1 and R1), one for the middle frame bay sub-models (L2, C2 and R2), and one for the bottom frame bay sub-models (L3, C3 and R3). Within the pre-buckling region the sub-section cross-sectional area, length and material properties clearly define the structure's pre-buckling stiffness. It is worth noting at this stage that the effect of small deviations in panel geometry is clearly identified during this process. In this case the layout of the panel is not quite symmetric, with the bottom frame bay sub-section models (L3, C3, R3) being a half-inch shorter than the top sub-section models (L1, C1, R1). The corresponding increase in stiffness is clearly seen in Figure 12 with curves for L3, C3 and R3 having the steepest initial slope.

The post-buckling stiffness and failure loads of the top (L1, C1, R1) and bottom (L3, C3, R3) frame bay sub-models appear dissimilar. Two principal structural differences explain is behaviour. First the boundary conditions on the top and bottom frame bays are different, with either the top or bottom of the structure cast in cerrobends or restrained by a frame (note the stringer cross-sections are not symmetrical). The effect of boundary conditions is minimal within the initial unbuckled region, however within the post-buckled region the boundary conditions effect the buckling mode and therefore the post-buckling stiffness and failure load. The second difference is the frame bay length, this quite clearly will change the initial stiffness of the curves, however in addition the variation in structural length will influence the buckling mode shape and again will affect the predicted post-buckling stiffness and failure load.

The middle frame bay sub-section models predict a stringer local-flexural buckling failure mode for the panel. The predicted load versus axial deflection data is then used to create the load response data for the non-linear springs to be used in the global spring framework model. The final stage is then the assembly of the sub-section springs to form the global model. Figure 13 schematically illustrates the global spring model. The global model in this case is loaded and constrained to replicate the specimen's mechanical test set-up, in order to benchmark global model accuracy.

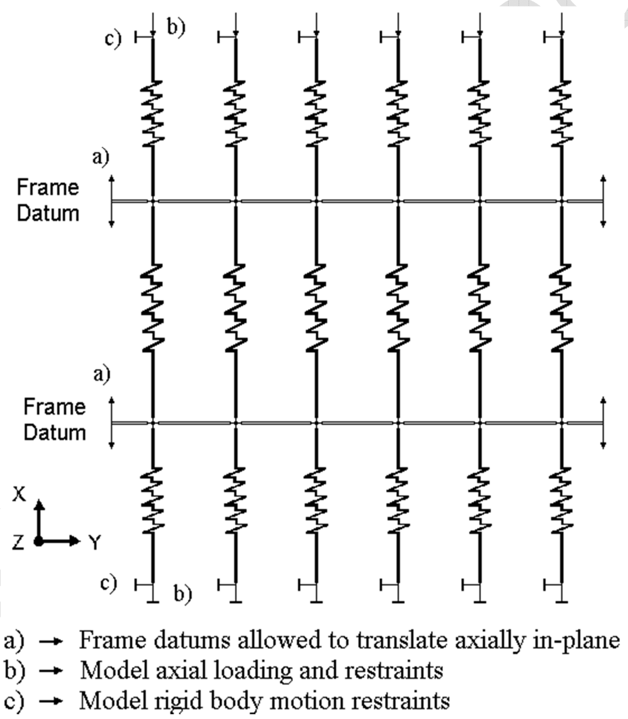


Figure 13 – Global spring framework model

## 5 Results

The global model stiffness results are presented in Figure 14 along with the experimental results and detailed 3D-Shell FE results. Table 1 presents the computation cost of both the efficient and detailed specimen FE models.

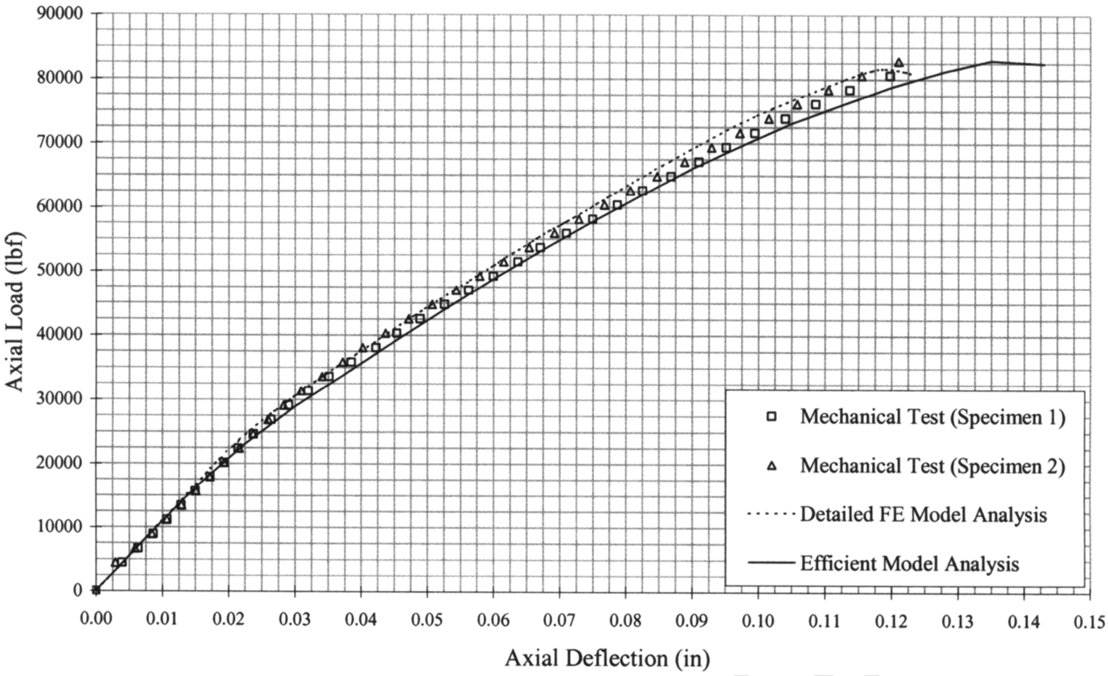


Figure 14 – Global model results

Figure 15 – Experimental failure mode

Two specimens were tested to failure. Based on the experimental stiffness curves local specimen skin buckling occurs at approximately 25,000 lbf and specimen failure occurs at 80,640 lbf for Specimen 1 and 82,880 lbf for Specimen 2. Both specimens fail through the same mechanism of stringer local-flexural buckling, ending in a convex specimen collapse (specimen skin side curving out, stringer side curving in, Figure 15). The experimental specimen's post failure stiffness data was not captured during the tests, therefore no negative slope is seen at the end of the experimental curves, Figure 14. The detailed FE model predicts local buckling at approximately

22,550 lbf, some 10% lower that the experimental value. The FE model however predicts the same stringer local-flexural failure mode as seen in the tests and predicts failure at a load of 81,741 lbf, 1.37% lower than Specimen 2 and 1.37% higher than Specimen 1. The detailed FE model stiffness output closely matches the experimental pre buckling gradient, and slightly over predicts the post buckling value. Due to the high predicted post buckling stiffness the FE model also slightly under predicts the specimen's axial deflection at failure. Again based solely on the load versus axial deflection curves the efficient global model predicts the specimen's local buckling load at approximately 23,750 lbf, 5% lower that the experimental value. The efficient model accurately predicts the structure's pre buckling stiffness and slightly under predicts the post buckling stiffness, as expected. The model predicts the failure load as 83,038 lbf, 2.9% higher than Specimen 1. Due to the under prediction of specimen post buckling stiffness and the over prediction of specimen failure load the model also over predicts the specimens axial deflection at failure. The efficient model predicts specimen stiffness within 5% of experimental values up to 85% failure load, and within 7.5% up to 95% failure load.

Comparing the model size (Degrees Of Freedom – DOFs) for the full specimen model and a single sub-model, Table 1 and the required analysis space (temporary analysis file size plus executable size) and time (wallclock time), it is clear that there is a non-linear relationship between model size and model cost when modelling non-linear buckling collapse behaviour. Considering the size of temporary analysis files and analysis executables, the full specimen model requires an expensive UNIX server box for its analysis, whereas the sub-models and global spring model could have been analysed on a much less expensive desktop UNIX box or PC. The total time required to build all 9 sub-models and the global spring model was 1.5 man-days, half the time required to build the full specimen model. Finally the total wallclock analysis time for the efficient modelling procedure was 1,124 sec, compared to 21,317 sec for the analysis of the full specimen model. This shows a possible reduction in compute time of 95%.

| | Model database size (MB) | Number of model DOFs | Input file size (MB) | Temporary analysis file size (MB) | Analysis increments | Analysis iterations | Analysis executable size (MB) | Wallclock time (sec) | Output file size (Total) (MB) |
|---|---|---|---|---|---|---|---|---|---|
| Detail FE Model | 10.97 | 90852 | 3.32 | 88.6 | 61 | 212 | 178.6 | 21317 | 231.4 |
| Efficient Model (Sub-sections) | | | | | | | | | |
| *L1* | 1.97 | 4524 | 0.15 | 4.73 | 43 | 120 | 18.2 | 89 | 5.33 |
| *C1* | 2.32 | 7740 | 0.24 | 4.74 | 36 | 103 | 18.2 | 73 | 4.60 |
| *R1* | 1.86 | 4140 | 0.14 | 4.73 | 38 | 114 | 18.2 | 87 | 4.80 |
| *L2* | - | 4524 | 0.15 | 9.25 | 56 | 162 | 24.9 | 248 | 11.36 |
| *C2* | - | 7740 | 0.24 | 9.26 | 35 | 111 | 24.9 | 136 | 7.75 |
| *R2* | - | 4140 | 0.14 | 9.25 | 55 | 199 | 24.9 | 254 | 11.18 |
| *L3* | - | 4524 | 0.15 | 4.15 | 40 | 129 | 17.3 | 83 | 4.58 |
| *C3* | - | 7740 | 0.24 | 4.16 | 36 | 120 | 17.4 | 70 | 4.35 |
| *R3* | - | 4140 | 0.14 | 4.15 | 26 | 134 | 17.3 | 56 | 3.23 |
| (Spring model) | 1.94 | 120 | 0.006 | 0.68 | 20 | 20 | 12.6 | 28 | 0.25 |
| Total | 8.09 | 49332 | 1.63 | 55.1 | - | - | - | 1124 | 57.4 |

*All pre and post processing performed on a SGI Octane™ with a 250 MHz R10,0000 processor and 512 MB of RAM. All analysis preformed on a Sun Enterprise™ 3500, with six 400 MHz UltraSPARC II™ processors and 6,144 MB of RAM.*

Table 1 – Computational analysis cost parameters

## 6 Conclusion

The driving force behind the work presented here is to increase the fidelity of global load models used in the aerospace industry. Presently global load models are highly idealised, with a single element representing a panel skin bay or a stringer section between frames. The aim here is to add to the global load model accuracy by accounting for the non-linear behaviour present due to the design philosophy of the structure. A typical global load model will be considered for in excess of 200 load cases and will consist of hundreds of thousands of degrees of freedom. As hardware developments have reduced run times for each loading case, airworthiness issues have increased the number of cases to be considered, resulting in an equilibrium for modelling fidelity, time and cost. In addition, each global loads model requires many man years to build at the present idealisation level, to try and model the entire structure at a higher level would greatly increase project timeframes and cost. Therefore, intelligent modelling procedures are required to increase model accuracy. The work presented aims to develop efficient modelling techniques to improve global model accuracy by accounting for sub-section non-linear behaviour without incurring the time penalty which comes with more detailed models. A simple non-linear sub-structuring strategy has been presented and results show great potential in increasing global model accuracy. The non-linear global model results match experimental stiffness results closely, with the efficient model predicting specimen stiffness within 5% of experimental values up to 85% failure load, and within 7.5% up to 95% failure load. Considering traditional global fuselage barrel models only account for linear behaviour this is a potential step forward for the accuracy of these models. The simple non-linear spring modelling strategy may also be used to reduce the required effort to built and run a complex 3D-Shell model of a stiffened panel structure. The modelling strategy reduces analysis run times but also reduces analysis job sizes therefore reducing the computational power required and consequently reduces the cost of required computational hardware.

Considering the potential of the modelling strategies introduced there are still a number of issues requiring investigation. The first is the development of additional strategies to accurately and efficiently model the non-linear behaviour of the structure when loaded in shear or combinations of compression and shear. Secondly considering the cost saving with respect to large detailed non-linear FE models, can the developed modelling methods be used along with mixed element coupling procedures [20] to reduce the cost of large structure FE modelling, with the use of developed sub-structuring or sub-modelling techniques.

**Acknowledgements**

The authors wish to thank both the Engineering and Physical Sciences Research Council (EPSRC–GR/R12749/01) and the Industrial Research and Technology Unit (IRTU–ST-198) for their financial assistance, as well as Gary Moore, Ken Poston and Derek Cottney for their technical support.

## References


1. Bruhn E F. Analysis and Design of Flight Vehicle Structures. 1st edition, Tri-State Offset Company, 1973.
2. NASA. NASA Astronautics Structures Manual. Vol. 3, 1961.
3. ENGINEERING SCIENCES DATA UNITS. Structures Sub-Series. ©ESDU International Ltd.
4. Lynch C J. A Finite Element Study of the Postbuckling Behaviour of a Typical Aircraft Fuselage Panel. PhD Thesis, Queen's University Belfast, Belfast, N. Ireland, 2000.
5. Murphy A. Accurate and efficient buckling and post buckling analysis of fuselage panels loaded in shear and compression. PhD Thesis, Queen's University Belfast, Belfast, N. Ireland, 2002.
6. Domb M M, Elliott W G, Leigh B R. Modelling of stiffener Crippling Phenomena Using Finite Element Analysis. Canadian Aeronautics and Space Journal, Vol. 44, No. 4, pp 256-262, 1998.
7. Dougherty J D, Padovan J, Srivatsan T S. Fatigue crack propagation and closure behaviour of modified 1070 steel: finite element study, Volume 56 Part 2 pp 189-212, Engineering fracture mechanics, 1997.
8. Geiro A, Grundy P, Cannon S, Nguyen V. Advanced finite element techniques for hull structural analysis, Proceeding of the eighth international offshore and polar engineering conference, Montreal, Canada, 1998.
9. Giglio M. FEM submodelling fatigue analysis of a complex helicopter component, Volume 21 pp 445-455, International journal of fatigue, 1999.
10. Cook R D, Malkus D S, Plesha M E. Concepts and applications of finite element analysis, 3rd edition, John Wiley & Son Inc., 1989.
11. Wang J T, Ransom J B. Application of interface technology in non linear analysis of a stitched/RFI composite wing stub box, AIAA-97-1190, AIAA/ASME/ASCE/AHS/ASC Structures, Structural Dynamics, and Materials Conference and Exhibit, Kissimmee, US, 1997.
12. Nemeth M P, Britt V O, Collins T J, Starnes J H. Non linear analysis of the space shuttle superlight weight external fuel tank, NASA-TP-3616, NASA, 1996.

13. Murphy A and Price M. Efficient Finite Element Modelling of Buckling and Post-Buckling Behaviour of Flat Stiffened Panels. NAFEMS World Congress 2001, Lake Como Italy, 2001.
14. Wittenberg T C, van Baten J J, de Boer A. Design of fibre metal laminates shear panels for ultra-high capacity aircraft, Volume 4 pp 99-133, Aircraft Design, 2001.
15. Lynch C, and Sterling S G. A Finite Element Study of the Postbuckling Behaviour of a Flat Stiffened Panel. 21st ICAS Congress, Melbourne Australia, ICAS-98-7,7,3, 1998.
16. Apicella A, Armentani E, Cali C, Caputo F, Esposito R. Buckling and post buckling analysis of a GLARE thick flat side panel, Proceeding of ETCE/OMAE 2000 joint conference energy for the new millennium, New Orleans, US, 2000.
17. Anonymous. ABAQUS / Standard User's Manual. Version 6.1, Hibbitt, Karlsson and Sorenson, 2000.
18. Becker A A. Understanding non-linear finite element analysis - Through illustrative benchmarks, 1st edition, NAFEMS (ISBN 1-8743-7635-2), 2001.
19. Niu M C. Airframe Structural Design. 1st edition, Hong Kong Conmilit Press Ltd, 1988.
20. McCune R W, Armstrong C G, Robinson D J. Mixed Dimensional Coupling in Finite Element Models. International Journal of Numerical Methods in Engineering, Vol. 49, pp 725-750, 2000.